Journal of Energy Storage 141 (2026) 119488

Contents lists available at ScienceDirect

Journal of Energy Storage

journal homepage: www.elsevier.com/locate/est

Research papers

A net energy gain framework for optimizing heat exchanger architectures in solid-state hydrogen storage systems

Wenpeng Hong [a], Ruixuan Wang [a], Mingjun Liao [a], Jianghao Cai [b], Fangfang Xie [a,*], Weijie Yang [b,*]

[a] School of Energy and Power Engineering, Northeast Electric Power University, Jilin, 132012, China
[b] Department of Power Engineering, School of Energy, Power and Mechanical Engineering, North China Electric Power University, Baoding, 071003, China

ARTICLE INFO

Keywords:
Hydrogen storage
Heat exchanger design
Net energy gain (NEG)
Thermal performance evaluation
Solid-state hydrogen systems

ABSTRACT

Efficient thermal integration is a critical bottleneck in energy-intensive systems such as solid-state hydrogen storage, where internal heat exchanger design governs both reaction kinetics and net energy efficiency. Existing evaluations, however, rarely couple thermal performance with the auxiliary energy required for system operation, limiting their applicability across technologies and scales. This study introduces a Net Energy Gain (NEG) framework as a unified performance indicator that integrates enthalpy change, pump work, storage volume, and reaction progress. The method is validated using four representative heat exchanger geometries, including spiral tubes, jacketed walls, straight-tube arrays, and fin-enhanced designs, across operating pressures of 6–20 bar. Results show that while finned structures reduce hydrogenation time by up to 35 % at 6 bar, they incur NEG penalties of ~10 J/s, whereas compact geometries sustain positive NEG values across the full pressure range, peaking at 15.75 J/s at 8 bar. NEG trends exhibit a non-monotonic dependence on pressure, revealing an optimal 10–12 bar window for balancing speed and efficiency. Guided by these insights, a new spiral-fin design was developed that achieves significant time reductions with minimal NEG loss, demonstrating the capability for structure-performance co-optimization of the framework. Beyond hydrogen storage, the NEG concept is architecture-agnostic, material-independent, and applicable to diverse thermal energy systems, offering a scalable methodology for maximizing net energy yield in renewable integration, energy conversion, and storage applications.

1. Introduction

Solid-state hydrogen storage constitutes a critical domain within hydrogen energy utilization [1], finding extensive application in hydrogen-powered vehicles [2], hydrogen energy transportation systems [3–7], hydrogen fuel cells [8–11], and the integration of hydrogen with [12–14]. A key component in these systems is the solid-state hydrogen storage container, which serves both as a containment unit and a reaction site for hydrogen absorption and desorption processes. These processes are governed by strongly coupled heat and mass transfer mechanisms in porous media, posing significant engineering and thermodynamic challenges. However, despite extensive efforts to improve heat and mass transfer performance, current research lacks a standardized framework for evaluating the energy efficiency of different container configurations under varying operational conditions. Addressing this gap is essential for guiding the rational development of hydrogen storage technologies.

In this context, existing investigations into solid-state hydrogen storage containers primarily examine the influence of structural configurations such as finned tubes, spiral tubes, and phase change material (PCM) coatings [15–20] and operational parameters such as pressure, temperature, and thermal conductivity [21–25] on the hydrogen uptake and discharge kinetics. A majority of these studies employ modeling and experimental validation of various structures as a foundation to explore container properties such as hydrogen absorption/desorption rates and reactor temperature distributions under varying pressure and temperature conditions. For instance, Vivek et al. [26] modeled a 60 kg $LaNi_5$ alloy multi-tubular hydride reactor to investigate structural effects on large-scale hydrogen storage system performance. The 90 % hydrogen absorption times for configurations with 7, 14, and 19 tubes were 985 s, 404 s, and 317 s, respectively. The introduction of longitudinal fins within the tubes further enhanced hydrogen absorption/desorption

* Corresponding authors.
E-mail addresses: xiefang705@163.com (F. Xie), yangwj@ncepu.edu.cn (W. Yang).

https://doi.org/10.1016/j.est.2025.119488
Received 14 September 2025; Received in revised form 21 October 2025; Accepted 11 November 2025

performance, demonstrating that both increasing tube count and incorporating fins significantly improve reactor efficiency. Wang et al. [27] leveraging electromagnetic dissipation principles, deduced the optimal fin shape for a cylindrical reactor to be a pin fin structure. By varying fin thickness, fin spacing, and reactor radius, they found that the pin fin reactor reduced hydrogen uptake time by 19.1 % compared to conventional uniform-thickness fins. Krishna et al. [28] designed a novel bionic leaf-vein fin structure for metal hydride reactors and proposed two new reactor designs based on it: a center straight tube and a narrow trapezoidal tube. These designs provided superior heat transfer and temperature uniformity, achieving 90 % reaction completion in 210 s, 145 s, and 80 s for the base fin structure versus the two novel structures, respectively. Ankush et al. [29] conducted numerical simulations of a concentric cylindrical reactor utilizing magnesium (Mg) as the hydrogen storage alloy and encapsulated sodium nitrate as the PCM. The addition of copper fins within the MH and PCM regions and the investigation of their effect on hydrogen absorption by varying fin number, thickness, and spacing revealed that reactors with 10 and 30 fins required 86.5 % and 97.3 % less time for hydrogen uptake, respectively, compared to the finless configuration. These findings collectively demonstrate that appropriate structural design, including tube arrangement and fin geometry, can substantially enhance heat and mass transfer, thereby accelerating hydrogen absorption.

However, beyond structural optimization, material-level thermal management also plays a critical role. The heat transfer process within different regions of the hydrogen storage container during the reaction is particularly complex, involving multiple mechanisms such as conduction, porous media heat transfer, and phase transition heat transfer. Variations in thermal conductivity significantly impact the hydrogen storage reaction kinetics. Praveen et al. [30] employed graphene oxide (GO), a novel two-dimensional material, to enhance the heat transfer performance of an MH reactor for faster hydrogen storage rates in $LaNi_5$. Results indicated that the addition of 1 *wt*% GO yielded relatively superior heat transfer, reducing reaction time by 61.7 % and achieving 90 % hydrogen storage capacity under comparable conditions. Atalmis et al. [31] increased the thermal conductivity of the metal hydride by incorporating expanded natural graphite (ENG) particles and copper additives, achieving a 3.5-fold increase which substantially reduced reaction time. Serge et al. [32] numerically investigated the H_2 charging and discharging process of a metal hydride tank filled with $LaNi_5$ and equipped with a paraffin wax (RT35) PCM jacket. By varying the thermal conductivity of both $LaNi_5$ and the PCM, they demonstrated that higher conductivities led to a significant reduction in reaction time. Mohamed et al. [15] designed three metal hydride beds to evaluate whether enhanced heat transfer and the addition of high-conductivity materials could improve hydrogen storage and release performance. Their results showed that increasing the heat transfer coefficient from 100 to 3000 $W/(m^2 \cdot K)$ reduced the hydrogen storage time from 668 s to 344 s, while the release time showed a smaller reduction, decreasing from 372 s to 246 s. These studies collectively indicate that improving the thermal conductivity of the storage medium through additive materials or structural modification can effectively enhance hydrogen absorption rates and facilitate more efficient heat management during operation.

In addition to improving thermal conductivity through material modification, operating temperature also plays a crucial role in governing heat transfer behavior and reaction kinetics. As an exothermic process, the initial reaction temperature significantly influences the performance of solid-state hydrogen storage containers. Tong et al. [33] employed temperature as a key variable in their analysis of the temperature distribution with a coiled-tube during hydrogen absorption, demonstrating that a 20 K temperature differential effectively mitigated localized high-temperature regions within the metal hydride. Atef et al. [34] developed a two-dimensional mathematical model to investigate heat transfer phenomena during hydrogen absorption in a large-scale metal hydride storage reactor. Their results indicated that elevated operating bed temperatures impair heat transfer efficiency within the container and consequently diminish the reaction kinetics of the hydrogen storage metal. Seyed et al. [35] modeled and optimized the transient behavior in a two-dimensional metal hydride storage tank, selecting the PCM initial temperature as the optimization variable for hydrogen uptake. Their findings revealed that reducing the initial temperature from 293 K to 273 K increased the reaction rate by 33 %. Cherif et al. [36] conducted numerical simulations on a $LaNi_5$ hydrogen storage reactor to characterize the temperature distribution across various reactor sections and elucidate the impact of heat transfer dynamics. Their simulation indicated that lowering the initial metal temperature does not affect overall storage capacity but facilitates a more rapid return to thermal equilibrium post-reaction. Chang et al. [37] investigated the influence of parameters including inlet coolant temperature, hydrogen pressure, and flow rate on hydrogen charging/discharging kinetics, utilizing a multi-spiral finned heat exchanger. Given that hydrogen absorption is exothermic and desorption is endothermic, lowering the operational temperature enhanced the absorption rate by 20 %, while increasing it accelerated the desorption rate by 25 %. Singh et al. [38] investigated the absorption performance of a cylindrical hydrogen storage system by adjusting the inlet temperature, revealing that at 288 K the system achieved 1 wt% hydrogen uptake within 560 s. Yuan et al. [39] modeled a spiral mini-channel reactor to study the influence of hydrogen inlet temperature on heat and mass transfer characteristics. Their results showed that the maximum hydrogen storage capacity was achieved near 318 K, with limited variation between 303 K and 333 K. These results highlight the sensitivity of hydrogen absorption and desorption dynamics to thermal boundary conditions. In addition to temperature, pressure represents another critical operating parameter that governs reaction kinetics and energy behavior in hydrogen storage systems.

Among investigations employing pressure as a variable parameter, Jing et al. [40] developed a three-dimensional model of a metal hydride reactor integrated with salt hydrate phase change material (PCM) for thermal recovery. Their analysis of the influence of PCM operating pressure and metal hydride reaction pressure on reactor performance optimization revealed that increasing the operating pressure accelerates the hydrogen absorption kinetics. Specifically, raising the pressure from 6 bar to 10 bar reduced the reaction completion time by 24 %. Lewis et al. [16] studied heat transfer processes during hydrogen absorption in a phase-change hydrogen storage reactor, utilizing inlet hydrogen pressure as the variable. They reported that elevated pressure progressively shortens the reaction duration but concomitantly induces a significant rise in the metal hydride reaction temperature. Afzal et al. [41] designed a heat exchanger based on a hexagonal honeycomb structure. Increasing the pressure from 15 bar to 40 bar resulted in a 22 % reduction in reaction time. Miled et al. [19] modeled a novel reactor incorporating PCM to store absorption heat for subsequent release during desorption, specifically examining the impact of pressure variations on absorption and desorption dynamics. Their simulations demonstrated that higher pressures substantially decrease reaction time while increasing the reaction temperature. Wang et al. [42] implemented a branch-tube microchannel heat exchanger. Upon increasing the pressure incrementally from 5 bar to 25 bar, the reduction in reaction time was non-uniform, exhibiting a difference of 170 s between the reductions achieved in the 5–10 bar and 20–25 bar intervals. Avik et al. [43] investigated a large-scale hydrogen storage reactor under different hydrogen supply pressures. Their findings indicate that supply pressure critically governs the absorption rate; however, excessive pressure significantly elevates the internal container temperature. This phenomenon is attributed to the conversion of increased hydrogen molecule kinetic energy into thermal energy, thereby heating the metal hydride.

Although previous studies provide valuable insights into the enhancement of heat exchangers, they are often limited to isolated structural configurations or narrow parametric scopes, lacking a generalized framework for energy performance evaluation. To address

this gap, the present study proposes a unified evaluation index based on Net Energy Gain (NEG), which simultaneously accounts for hydrogen absorption kinetics and auxiliary power consumption. Specifically, the NEG framework is designed for cross-structural and cross-scale evaluation of energy efficiency in solid-state hydrogen storage reactors that incorporate various internal heat-exchanger configurations, such as spiral tubes, fins, and baffle-enhanced designs. It provides a quantitative metric to assess the balance between effective hydrogen absorption and additional energy consumption under different operating pressures and heat supply conditions. Physically, NEG represents the economy of hydrogen absorption by hydrogen storage materials per unit mass, and the variation of this economy among distinct structures can be reflected through changes in system parameters. This framework is particularly suited for thermally coupled metal hydride systems applied in renewable energy integration, energy conversion, and storage scenarios, offering a system-level criterion for practical design optimization.

The overall research structure and methodology are illustrated in Fig. 1, which outlines the conceptual foundation, model development, parametric evaluation, and performance validation steps. In this framework, pressure is treated as the primary operational variable, and the enthalpy evolution during hydrogen absorption is analyzed to define a cumulative NEG that quantifies effective energy output. Four representative internal heat exchanger configurations are examined using a two-dimensional axisymmetric model to investigate how structural variations influence energy performance. A sensitivity analysis is further conducted to assess the model's robustness across a range of pressure conditions. This NEG-based framework not only bridges a key gap in the current hydrogen storage system design methodology, but also offers a scalable theoretical foundation for optimizing energy-efficient heat exchanger structures in practical applications.

2. Development and conceptual validation of the NEG Model

2.1. Evaluation rationale and data basis

To establish a comprehensive framework for evaluating performance and energy efficiency in solid-state hydrogen storage systems, this study first analyzes representative exchanger configurations and material systems documented in the literature [44,45]. Particular attention is given to $LaNi_5$, which is selected as the working material due to its low hydrogenation temperature, high reversibility, and activation-free behavior. These characteristics not only contribute to its widespread application in practical systems but also ensure reliable, consistent data for model development. A complete list of literature sources used for model construction is provided in the Supporting Information of Table S1.

In solid-state hydrogenation, both pressure and temperature critically influence heat exchanger performance. However, pressure is typically the more dominant factor, exerting a stronger effect on both hydrogen uptake kinetics and auxiliary energy input. Based on this, our analysis focuses primarily on pressure-dependent system behavior. As summarized in Fig. 2, four representative internal heat exchanger configurations are identified from existing $LaNi_5$-based studies: (a) spiral tubes, (b) jacketed walls, (c) straight-tube arrays, and (d) finned structures. These configurations vary in thermal transport characteristics and exhibit distinct trade-offs between heat transfer enhancement and power consumption.

Despite numerous efforts to optimize such exchangers, existing evaluation approaches remain fragmented, as they often focus on specific operating conditions or rely on single-objective metrics. As a result, cross-comparisons among designs are limited by inconsistent assumptions, boundary conditions, and performance priorities. To address this challenge, we propose a unified performance indicator that incorporates both energy input and system response across varying pressures. This integrated metric lays the foundation for the NEG model introduced in the following section.

2.2. Thermodynamic derivation of the NEG model

To quantitatively evaluate the energy efficiency of hydrogen storage containers under varying operational pressures, a thermodynamic framework is constructed. The core idea is to quantify both the energy output from hydrogen uptake and the auxiliary energy input required to sustain the reaction. A stepwise derivation is presented below.

The analysis begins with the definition of the mass-based hydrogen storage fraction, which serves as a dimensionless indicator of hydrogen uptake [42]. It is expressed as:

$$wt\% = (m_a - m_b)/m_b \tag{1}$$

where m_b is the mass of the metal hydride before absorption (g) and m_a is the mass after hydrogenation (g). Although this metric reveals the temporal evolution of hydrogen storage, it does not provide direct insight into energy efficiency, as it lacks physical units and cannot be compared to power consumption.

To bridge this gap, the effective work (W_e) is introduced as a measure of the recoverable energy released by the absorbed hydrogen. The calorific value of hydrogen is 71,500 J/g, W_e is computed as:

$$W_e = P_a \times m \times V \times 71500 \tag{2}$$

where P_a is the hydrogen mass adsorption rate (g/s), m is the fraction of hydrogen absorbed per unit volume of the metal hydride, and V is the

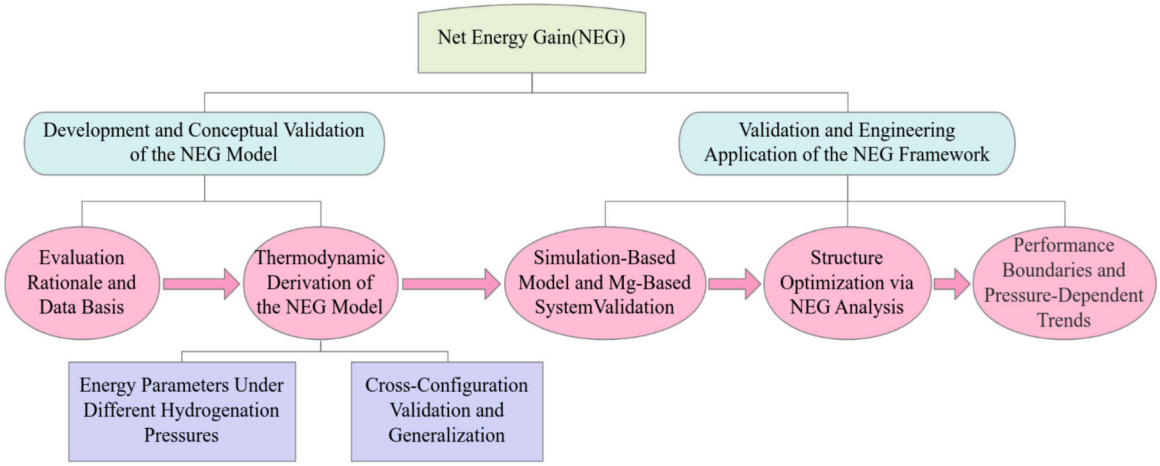

Fig. 1. Research workflow of the NEG-based evaluation framework.

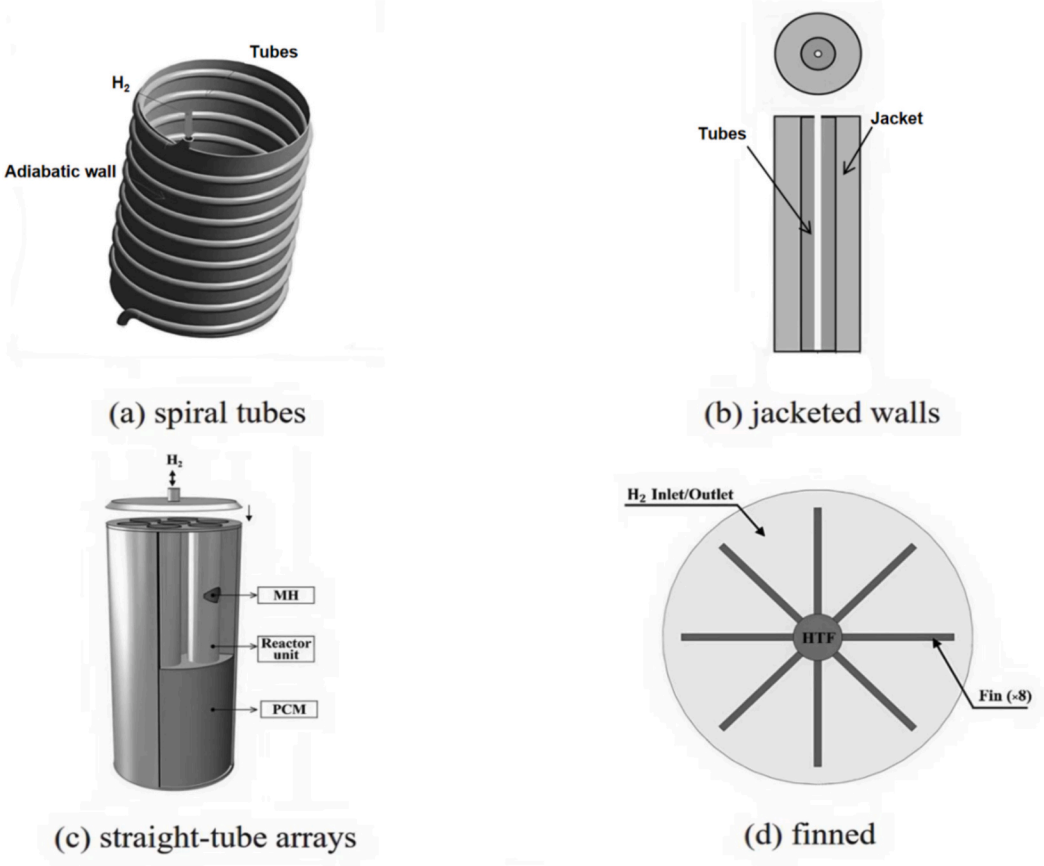

Fig. 2. Four different hydrogen storage heat exchanger configurations.

volume of the hydride bed (m^3). This formulation captures the energetic output of the system but does not reflect the auxiliary energy cost, as it omits the energy penalty required to drive absorption.

The cumulative input work (W_{in}) accounts for this cost and includes power consumed by the hydrogen pressurization and coolant systems. Assuming constant power operation, W_{in} is computed as:

$$P_g = p_{in} \times V = m \times V_m \times p_{in}/\eta_g \tag{3}$$

$$P_l = p_{in} \times S \times V_f/\eta_l \tag{4}$$

$$W_{in} = (P_g + P_l) \times t \tag{5}$$

where η_g and η_l represent the efficiency of the gas and cooling pumps, respectively, p_{in} represents the inlet pressure of hydrogen (bar), V_f represents the flow rate at the outlet of the cooling pump (m/s), S represents the cross-sectional area of the cooling pump tube (m^2), and V_m represents the volume per unit mass of hydrogen (g/L). It should be mentioned that since the efficiencies of the gas and coolant pumps are empirical parameters that are seldom reported in the literature, representative nominal values of $\eta_g = \eta_l = 0.70$ were adopted according to typical engineering ranges of small-scale hydrogen circulation and compression systems. Sensitivity tests showed that variations within ±10 % of these values do not affect the overall P_{net} and *NEG* trends.

Combining these two metrics, the net work W_{net} is then defined as:

$$W_{net} = W_e - W_{in} \tag{6}$$

This indicator reflects the net energy recoverable from the storage process. W_{net} is defined as the difference between the calorific value of hydrogen (representing the theoretical maximum recoverable energy) and the auxiliary pump work, reflecting the net useful work performed by the storage system. While W_{net} is valuable for pressure sensitivity studies within a single system, it lacks generality across geometries. Structural parameters (e.g., surface area, flow path) alter both W_e and W_{in}, making W_{net} non-transferable.

To enable cross-configuration benchmarking, we define the net power (P_{net}) as the differential rate between energy output and input at a given reaction stage:

$$P_{net} = W_{net}/\bar{t} \tag{7}$$

where $\bar{t}$ represents the time required to reach different reaction scores. While P_{net} provides an effective assessment of instantaneous container performance at various stages of the reaction, significant variability in the data during the early phase of hydrogenation limits the ability to extract consistent and reliable trends. To obtain a smoother, geometry-independent performance metric, we introduce the Net Energy Gain (NEG), defined as the accumulated positive net power from the thermodynamic breakeven point (where P_{net}) onward:

$$x = \int (\Delta t \cdot P_{net}) \tag{8}$$

This metric captures the accumulated surplus energy from hydrogen absorption relative to input cost after the breakeven. Color-coded scatter plots visualize NEG across systems and pressures, revealing general trends in energy efficiency and system optimization. Together, the derivation of W_e, W_{in}, W_{net}, P_{net}, and NEG establishes a comprehensive thermodynamic framework for evaluating and comparing hydrogen storage container performance under pressure-driven conditions.

2.3. Transient energy dynamics and efficiency degradation under varying pressures

To further evaluate the NEG model's applicability under realistic

operating conditions, we analyze the time-dependent evolution of energy parameters (W_e, W_{in}, and W_{net}) under different hydrogenation pressures. As shown in Fig. 3a, the hydrogen storage fraction increases nearly linearly during the initial and mid-reaction stages, indicating steady hydrogen uptake. As shown in Fig. 3b, this behavior is mirrored by the effective work W_e which is directly proportional to the absorbed hydrogen mass. In contrast, the cumulative input work W_{in} (Fig. 3c) grows more steeply at higher pressures due to increased compression and cooling demands. Consequently, in Fig. 3d, the net work W_{net} initially rises but later declines, as hydrogen uptake slows while auxiliary power input continues to accumulate. This shift in trend marks the thermodynamic breakeven, indicating the onset of energy inefficiency as the auxiliary input continues to rise while the hydrogen uptake slows down.

While time-based analysis provides intuitive insight into energy accumulation and dissipation, it is inherently constrained by reaction duration and structural scale, which limits its generalizability across different systems. To address this, Fig. 4 redefines the independent variable as the reaction fraction, thereby decoupling the analysis from temporal progression. This reframing enables more universal benchmarking and reveals performance features that time-based plots may obscure.

As shown in Fig. 4, net power P_{net} exhibits a characteristic three-phase pattern: it initially rises (0–25 % reaction), peaks during moderate hydrogenation (25–45 %), and subsequently declines to negative values beyond 45 %. This pattern arises from fast initial uptake, pressure-driven acceleration in the mid-stage, and reduced absorption at later stages due to saturation, with auxiliary systems running continuously throughout the process.

This three-phase behavior stems from distinct underlying physicochemical mechanisms. In the initial phase (0–25 %), hydrogen uptake is rapid due to abundant active sites on the metal hydride surface, and the energy output rate (effective work) exceeds the auxiliary power input, resulting in positive P_{net}. However, under higher pressures, elevated local temperatures induced by exothermic absorption begin to offset the reaction rate. In the intermediate phase (25–45 %), higher hydrogen pressures enhance molecular flux and kinetic energy, temporarily accelerating absorption despite thermal inhibition. During this window, P_{net} reaches its peak, offering the best trade-off between speed and

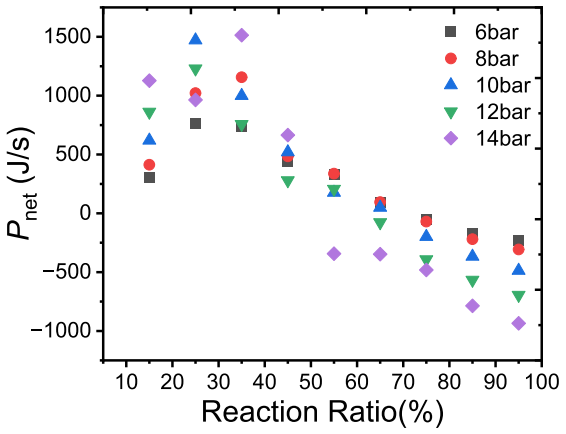

Fig. 4. P_{net} versus reaction fraction under different pressure conditions. Positive regions indicate net energy gain, while negative regions reflect an energetic penalty.

energy efficiency. When the reaction fraction exceeds 45 %, P_{net} becomes negative because the auxiliary pumping power surpasses the instantaneous hydrogen absorption heat. This reflects the gradual saturation of reaction sites and reduced thermal driving force at high conversion, leading to increased energy losses if the operation continues. In practical systems, this regime should be avoided to ensure energy-efficient operation. Most active sites become saturated, slowing the absorption kinetics. Nonetheless, the gas compression and cooling systems continue to operate at constant power, leading to rising energy costs without significant hydrogen gain. Although this divergence causes P_{net} to drop below zero, the hydrogen storage capacity at this point reaches only about 45 % of the maximum value. Thus, rather than terminating the reaction prematurely, the hydrogen supply and liquid-pump pressures can be optimized to maintain a positive P_{net}, balancing economic efficiency with storage completeness.

Although expressing P_{net} as a function of reaction progress enhances interpretability, it remains a stage-dependent and instantaneous metric. The strong sensitivity of P_{net} to early-stage fluctuations and its inability to capture cumulative system performance limit its utility as a

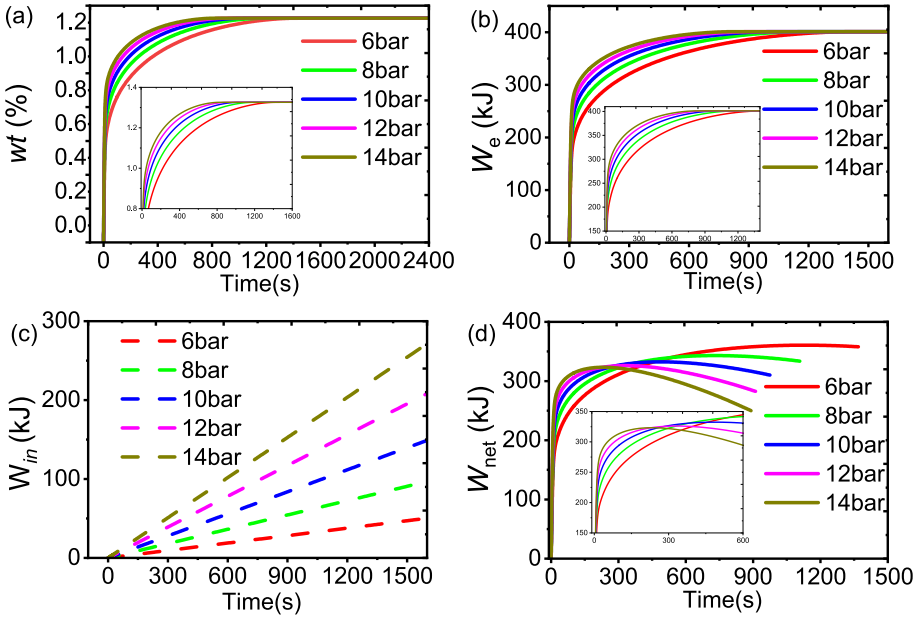

Fig. 3. Time evolution of key energy parameters under different pressure conditions: (a) mass-based hydrogen storage fraction *wt*%, (b) effective work W_e, (c) cumulative power input W_{in}, and (d) net work W_{net}.

standalone indicator. These limitations underscore the need for a more stable, integrative metric that accounts for the entire hydrogenation cycle and supports geometry-independent comparison. This motivates the introduction of the NEG indicator, which accumulates net power from the breakeven point onward and provides a robust basis for evaluating structural efficiency across different operating pressures. In the following sections, NEG will be applied to compare multiple heat exchanger configurations and validate its general applicability.

2.4. NEG validation across multiple structural configurations

Following the theoretical derivation and pressure-dependent validation of the NEG indicator, it is essential to assess its general applicability across structurally diverse hydrogen storage systems. To ensure comparability among datasets from different literature sources, only cases with consistent boundary conditions (hydrogen inlet temperature, porosity, and activation energy) were selected. All parameters were standardized to SI units, and NEG values were normalized with respect to system mass and volume, thereby ensuring that the observed trends reflect the intrinsic pressure-dependent behavior rather than variations in experimental setup. Structural independence is a fundamental requirement for any performance metric intended for cross-design benchmarking. This implies that the metric should maintain its reliability and clarity regardless of variations in geometry or topology. To this end, we evaluated the NEG trends across seven representative heat exchanger configurations extracted from the literature, under varying hydrogenation pressures.

Fig. 5 presents a consolidated NEG response map using color-mapped scatter plots, where each marker shape denotes a specific structural type and each color encodes the corresponding NEG value. Because the original data reported in the literature were derived under different simulation and boundary conditions, a certain degree of data deviation exists. Consequently, the scatter observed among structures of the same type does not indicate inconsistency in the overall NEG trend but reflects variations in model assumptions and parameter settings. Despite the heterogeneity in design and source data, all configurations exhibit a consistent trend: as pressure increases, hydrogenation response times shorten, while NEG values gradually decline. This behavior reflects the growing auxiliary energy burden associated with higher-pressure operation and confirms the thermodynamic validity of NEG as an integrated performance indicator.

To quantify these trends more rigorously, a nonlinear regression was performed using a power-law model ($y = a{\cdot}x^{b}$) to capture the pressure-dependent variation of NEG. This form offers better adaptability to the nonlinear scatter distribution and aligns with the theoretical relationship between reaction kinetics and pressure. The fitting results (Figs. 5a-5d) show high correlation coefficients ($R^2 > 0.95$), indicating reliable regression performance. In contrast, optimized designs such as coiled tubes and spiral fins exhibit much lower a-values, with a minimum of 556, indicating enhanced thermodynamic response and better adaptation to pressure changes. These results illustrate that NEG is not only sensitive to efficiency degradation trends but also effective in differentiating structural quality on a normalized basis.

More importantly, the NEG profiles as a function of pressure remain smooth and continuous for all configurations, forming clearly segmented trajectories across different pressure ranges without any abrupt transitions. This structural invariance strongly supports the geometry-agnostic nature of NEG. For instance, while jacketed walls and straight-finned tubes show steep NEG declines at elevated pressures, spiral-fin exchangers maintain both high NEG values and consistent energy-performance profiles, particularly within the 9–15 bar operating window.

Fig. 6 further compares the seven configurations by plotting pressure versus hydrogenation response time, with color-coded NEG overlays. Notably, the improved spiral-fin heat exchanger consistently maintains positive NEG values while achieving the shortest response times over the entire pressure range. This dual advantage highlights its suitability for pressure-driven system optimization.

A particularly insightful observation is the emergence of a NEG breakeven threshold around 20 bar, shared across all configurations. This point marks the onset of diminishing returns: additional pressure no longer improves hydrogen uptake but significantly increases energy

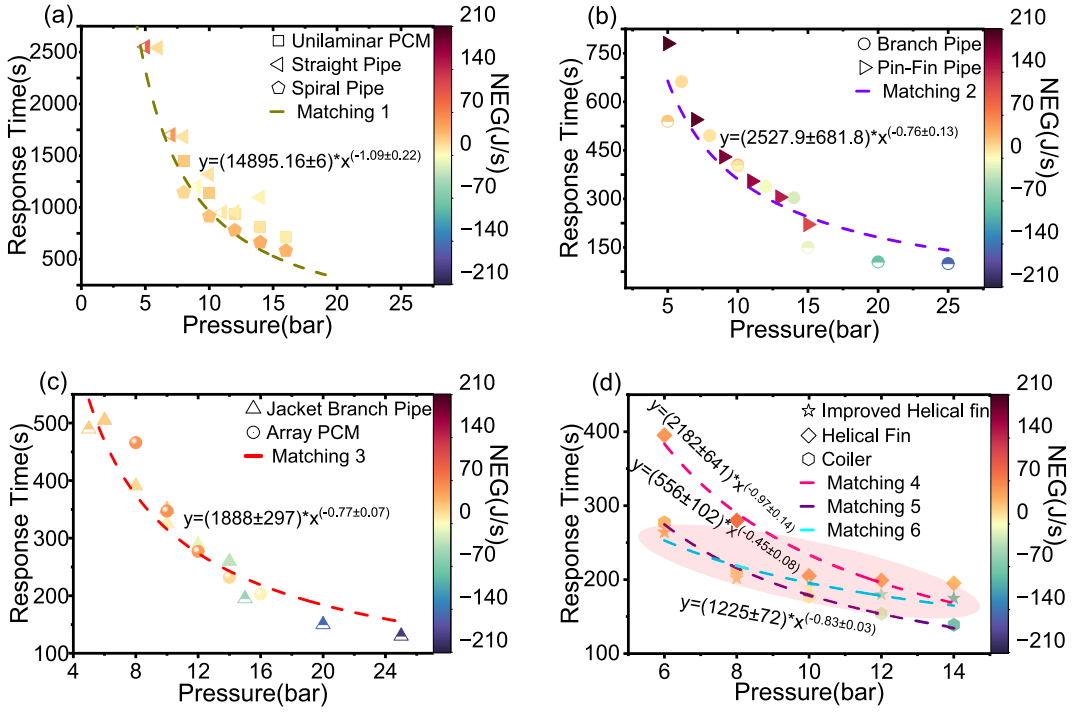

Fig. 5. Nonlinear regression fitting and NEG performance of structures with different degrees of optimization: (a) simple pipe structures; (b) complex pipe structures; (c) jacket wall structures; and (d)finned structures.

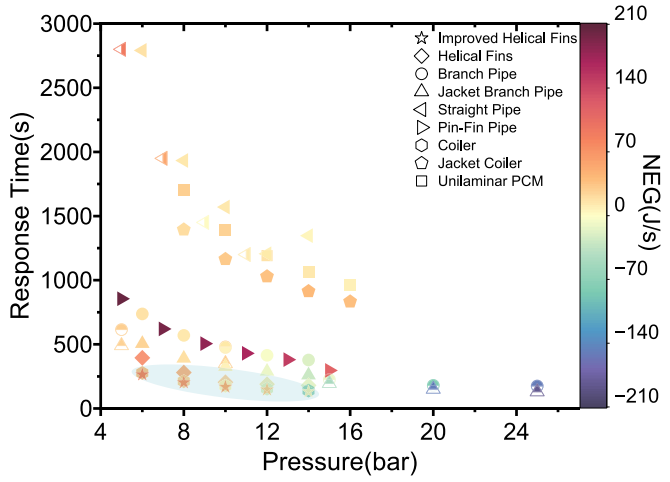

Fig. 6. Performance of improved spiral fins in all heat exchanger structures.

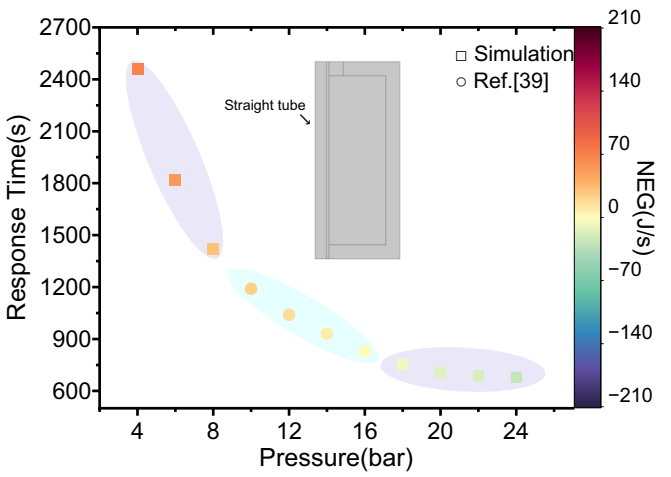

Fig. 7. Variation of reaction time and NEG with pressure for straight tube heat exchanger.

costs. The consistency of this threshold across structures reinforces the physical grounding of the NEG framework and its ability to capture system-level efficiency limits independent of geometric factors.

These findings collectively confirm that NEG serves as a reliable metric for assessing efficiency under variable pressures and supports fair benchmarking of heat exchanger performance regardless of structural differences. This universality enables broad application of NEG in design evaluation, operational planning, and system optimization for solid-state hydrogen storage systems.

Beyond its theoretical rigor, the NEG model holds substantial engineering value. By integrating hydrogen uptake kinetics with auxiliary energy consumption, it enables multi-objective optimization under real-world constraints. For systems operating under tight energy budgets, designs with modest capacity but high NEG values may be favored. Conversely, for scenarios requiring rapid hydrogenation, NEG helps quantify the trade-offs between speed and energy penalty. Furthermore, its applicability across material systems and design types makes it a powerful tool for rational structure selection, system planning, and standardized evaluation.

3. Validation and engineering application of the NEG Framework

3.1. Simulation-based model validation

To verify the accuracy and practical reliability of the proposed NEG framework, numerical simulations were conducted using a representative straight-tube heat exchanger configuration. A finite element model was developed in COMSOL, replicating a cylindrical solid-state hydrogen storage container constructed from aluminum, filled with $LaNi_5$ powder at a porosity of 0.5. The system was maintained at a constant hydrogen inlet temperature of 298 K, with geometric parameters adapted from literature benchmarks [46] (Fig. 7).

To assess model fidelity, simulation outputs were compared against published experimental datasets. The hydrogenation reaction time and the derived NEG values were identified as the two key metrics for performance validation. Pressures below 9 bar cause excessively long hydrogenation durations with negligible kinetic significance, whereas pressures above 20 bar may exceed the mechanical tolerance of the storage vessel and lead to model instability. Accordingly, the simulation was performed within 9–15 bar and 15–20 bar intervals to balance reaction rate, safety, and numerical stability. As summarized in Supporting Information of Tables S2 and S3, the simulated values closely tracked experimental results across all conditions. For example, at 8 bar, the simulated reaction time was 1400 s versus 1420 s from literature data, and the corresponding NEG was 15.75 J/s compared to 15.99 J/s. The small discrepancies (<1.5 %) between simulated and reference data mainly result from manual extraction and interpolation of published values, as well as minor uncertainties in boundary conditions and material properties. These differences are within the acceptable range for numerical verification, confirming the reliability of the model. Quantitative evaluation yielded mean relative errors of 1.32 % for reaction time and 1.12 % for NEG, indicating strong agreement and validating the physical and thermodynamic consistency of the simulation approach. These low deviations confirm that the NEG metric not only reflects theoretical efficiency trends but can also be reliably reproduced using numerical methods, thereby reinforcing its applicability in both predictive modeling and system optimization tasks.

3.2. Material transferability: Mg-based system validation

To further validate the material independence of the NEG metric, comparative analyses were conducted using magnesium-based hydrogen storage systems [47,48]. As shown in Table 1, the results extracted from prior studies demonstrate consistent pressure-dependent trends: with increasing pressure, both reaction time and NEG values decrease, in line with the behaviors previously observed in $LaNi_5$-based systems. For example, the NEG value shifts from +2.50 J/s at 10 bar to −30.74 J/s at 16 bar, while response time shortens from 605 s to 447 s. This consistency across different hydride materials supports the transferability of the NEG metric and highlights its robustness as a universal performance indicator applicable to multi-material hydrogen storage systems.

3.3. Performance boundaries and pressure-dependent trends

To evaluate the applicability of NEG in extreme operating conditions, extended simulations were conducted under two pressure regimes: low-pressure (4–6 bar) and high-pressure (18–24 bar) zones. The straight-tube configuration served as the base model [49]. Fig. 7 illustrates the variation of reaction time and NEG across these conditions, using a color gradient to represent NEG values from +210 J to −210 J.

At low pressures, reaction times increase substantially, and NEG values appear elevated at low pressures, but this reflects prolonged

Table 1
Reaction time and NEG values for Mg-based [29] storage container.

Pressure (bar)	10	12	14	16
Response Time (s)	605	533	483	447
NEG (J/s)	2.50	−7.82	−18.40	−30.74

energy input over extended durations rather than improved thermodynamic performance. The system becomes inefficient as the extended duration negates the marginal thermal benefit. Conversely, in the high-pressure regime, reaction times decrease but with diminishing improvement. NEG values continue to drop linearly, revealing an energy penalty that outpaces kinetic enhancement. These trends confirm the non-monotonic pressure dependency of NEG, validating its utility as a tool for rapid identification of optimal pressure windows.

The results further indicate that although heat transfer-enhancing structures (e.g., fins or tubes) can accelerate hydrogenation, they often incur additional auxiliary energy costs that erode net performance, particularly under higher pressure conditions. Thus, a performance-efficiency trade-off emerges. NEG effectively captures this balance by simultaneously accounting for hydrogen absorption kinetics and energy input burden, making it a suitable metric for multi-objective structural evaluations.

3.4. Structure optimization via NEG analysis

Building on the observed NEG-pressure trends and the identified optimal operation window, this part explores how the NEG metric can be applied to structural performance evaluation and the rational design of internal heat exchangers. First, we analyze the relationship between NEG variation and response time reduction in a baseline straight-tube heat exchanger configuration. Table 2 summarizes the rate of response time reduction per unit decrease in NEG across four pressure intervals. Results reveal a non-monotonic trend in energy-efficiency trade-offs: the 10–12 bar interval yields the highest efficiency gain (123.9 s per J/s reduction in NEG), while performance benefits diminish beyond this range. These findings suggest an optimal operating window of 10–12 bar for the straight-tube configuration, where pressure elevation yields the most favorable balance between hydrogen uptake kinetics and energy cost.

Guided by these insights, the improved helical-fin configuration (Fig. 8) is particularly suitable for rapid hydrogen charging and discharging scenarios such as in hydrogen fuel cells, mobile hydrogen-powered devices, or small-scale storage systems requiring high responsiveness. In contrast, for stationary applications emphasizing economic efficiency, lower-pressure operation is preferable. This analysis demonstrates that the proposed design effectively balances kinetic enhancement with practical operational demands. As shown in Table 3, the results show a substantial performance enhancement, especially under low-pressure conditions. For instance, at 6 bar, the hydrogenation time was reduced by 33 %, which from 395 s (literature baseline [34]) to 264 s, while the corresponding NEG value dropped by less than 5 % (from 70.8 to 67.3 J/s). This asymmetric gain, where a modest energy trade-off yields significant kinetic improvements, reflects the structure's efficiency under energy-constrained conditions. Moreover, even in the mid-pressure range (8–10 bar), the structure maintained a positive and stable NEG, demonstrating adaptability across operating conditions. The reduction in hydrogenation time achieved by the improved helical-fin structure outweighs the minor decrease in NEG, suggesting that the energy cost of enhancement remains economically acceptable. In fast-response scenarios such as hydrogen refueling or fuel-cell vehicles, operating at slightly higher pressure is advantageous to maximize throughput. In contrast, stationary energy-storage systems prioritize cost-effectiveness, where lower pressure operation is preferred to maintain economic efficiency. This comparison demonstrates the NEG framework's ability to quantitatively evaluate the trade-off between performance improvement and energy expenditure.

Table 2
Response time change per unit NEG reduction across pressure intervals.

Pressure (bar)	8–10	10–12	12–14	14–16
Time Reduction Factor (J/s)	85.8	123.9	28.7	28.2

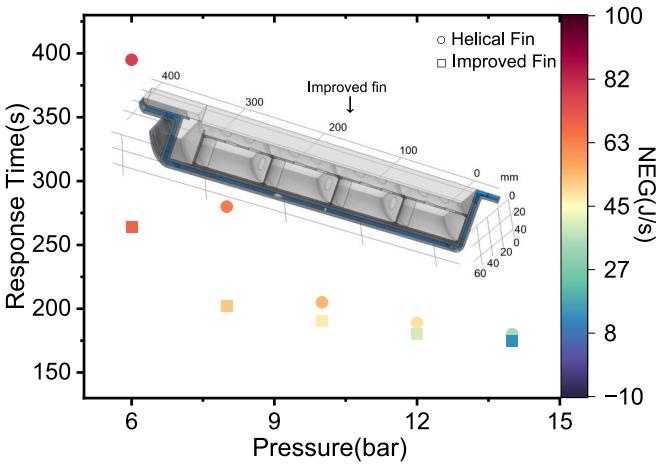

Fig. 8. NEG and reaction time versus pressure for improved fins versus spiral fins.

Table 3
Performance parameter comparison between fins of literature [37] and improved fins.

Pressure (bar)	Literature time (s)	Simulation time (s)	Literature NEG (J/s)	Simulation NEG (J/s)
6	395	264	70.8	67.3
8	280	202	62.1	60.1
10	205	190	52.8	44.3
12	189	180	43.3	30.0
14	180	175	29.9	11.7

Compared to previously reported spiral, pin-fin, and PCM-coated geometries, our design uniquely achieves both the shortest response time and a consistently positive NEG across the full pressure spectrum. This marks the first instance, to the best of our knowledge, of a hydrogen storage structure delivering dual-optimal performance in terms of energy and kinetics. Furthermore, the results illustrate that the NEG-based framework can go beyond analysis to actively inform the development of superior structural solutions. From model construction to structural application and system-wide validation, this section demonstrates a full-cycle NEG-driven design pathway. The proposed strategy is not only computationally accessible but also practically implementable. Given its robustness and scalability, the design is particularly well-suited for distributed hydrogen systems, portable energy modules, and applications where auxiliary power is limited. As such, it represents a versatile and high-performance template for the next generation of thermally integrated hydrogen storage systems.

3.5. Practical relevance and comparative advantages

Having demonstrated the value of NEG in guiding structural optimization and validating its practical engineering benefits, it is now essential to examine the broader significance of NEG as a unified performance metric. This section shifts focus from structural design outcomes to a methodological analysis of NEG's comparative strengths, evaluating how it outperforms conventional indicators under dynamic and complex conditions. Studies by Atef [36] and Mellouli [18] have reported that finned structures, while improving localized thermal performance, often result in increased system complexity, internal flow resistance, and parasitic heat losses. These adverse effects align with NEG-based results, wherein higher power inputs and reduced thermodynamic returns are penalized quantitatively. Thus, NEG provides a consistent interpretation of system-level efficiency beyond traditional heat transfer metrics.

Furthermore, compared to conventional evaluation criteria such as

COP (coefficient of performance) or steady-state thermal efficiency, NEG captures transient dynamics and energy overheads associated with auxiliary equipment. This makes the metric particularly relevant for compact and time-dependent systems. It also enables performance assessment under dynamically changing conditions, an aspect that is often overlooked by traditional indicators.

Nonetheless, the current implementation of the NEG model assumes quasi-steady operation and spatial uniformity in heat and mass distribution. While this provides analytical tractability, it may limit predictive power in large-scale or geometrically complex systems. Future developments could incorporate spatially resolved models and dynamic control inputs to enhance applicability.

In summary, the NEG metric exhibits strong agreement with both simulation and experimental data, performs consistently across different structures and materials, and reveals nuanced pressure-dependent trends. It holds substantial promise for guiding the design and optimization of solid-state hydrogen storage systems, especially in energy-constrained or performance-critical applications.

4. Conclusion

This study proposes a NEG-based evaluation framework as a unified metric for assessing heat exchanger performance in solid-state hydrogen storage systems. By integrating thermal effectiveness with auxiliary energy input, the NEG model enables system-level energy efficiency analysis across diverse structural configurations. Comparative simulations of four representative geometries, including U-shaped tubes, jacketed surfaces, straight-tube arrays, and fin-enhanced exchangers, demonstrate that the model effectively captures the balance between hydrogenation performance and associated energy consumption. While extended-surface designs accelerate absorption and increase storage capacity, they often incur higher energy penalties due to added thermal resistance or flow complexity. In contrast, compact or geometrically efficient structures achieve higher NEG by optimizing the balance between heat transfer gain and power input.

The NEG model aligns with experimental observations reported in the literature and complements traditional thermal performance metrics such as COP and energy efficiency. Crucially, it extends beyond steady-state evaluations by incorporating transient behavior, geometric compactness, and auxiliary load considerations. Although the current implementation assumes quasi-steady operation and uniform thermal distribution, the framework is inherently scalable. It provides a robust foundation for future enhancements involving dynamic heat-mass coupling, spatial heterogeneity, or material-specific thermophysical properties. More broadly, the NEG approach offers a generalized, transferable methodology for optimizing thermal integration in a wide range of energy-intensive technologies, including fuel cells, thermal batteries, and power-to-gas systems.

CRediT authorship contribution statement

Wenpeng Hong: Writing – review & editing, Validation, Conceptualization. **Ruixuan Wang:** Writing – review & editing, Writing – original draft, Visualization, Software, Investigation. **Mingjun Liao:** Writing – review & editing, Formal analysis. **Jianghao Cai:** Writing – review & editing. **Fangfang Xie:** Writing – review & editing, Supervision, Methodology, Funding acquisition, Conceptualization. **Weijie Yang:** Writing – review & editing, Supervision, Funding acquisition, Conceptualization.

Declaration of competing interest

The authors declare that they have no known competing financial interests or personal relationships that could have appeared to influence the work reported in this paper.

Acknowledgments

This study was supported by the National Natural Science Foundation of China (No. 52306074), the Natural Science Foundation of Hebei Province (E2023502006) and the Fundamental Research Fund for the Central Universities (2025MS131).

Appendix A. Supplementary data

Supplementary data to this article can be found online at https://doi.org/10.1016/j.est.2025.119488.

Data availability

Data will be made available on request.

References

[1] A. Kumar, P. Muthukumar, P. Sharma, E.A. Kumar, Absorption based solid state hydrogen storage system: A review, Sustain Energy Technol Assess 52 (2022) 102204.
[2] M. Peksen, Hydrogen technology towards the solution of environment-friendly new energy vehicles, Energies 14 (2021) 4892.
[3] R. Shi, X. Chen, J. Qin, P. Wu, L. Jia, The state-of-the-art progress on the forms and modes of hydrogen and ammonia energy utilization in road transportation, Sustainability 14 (2022) 11904.
[4] Z. Abdin, C. Tang, Y. Liu, K. Catchpole, Large-scale stationary hydrogen storage via liquid organic hydrogen carriers, iScience 24 (2021) 102966.
[5] B. Arslan, M. Ilbas, S. Celik, Experimental analysis of hydrogen storage performance of a LaNi5–H2 reactor with phase change materials, Int. J. Hydrog. Energy 48 (2023) 6010–6022.
[6] H. Ishaq, I. Dincer, C. Crawford, A review on hydrogen production and utilization: Challenges and opportunities, Int. J. Hydrog. Energy 47 (2022) 26238–26264.
[7] Z. Ding, Y. Li, H. Yang, Y. Lu, J. Tan, J. Li, et al., Tailoring MgH2 for hydrogen storage through nanoengineering and catalysis, Journal of Magnesium and Alloys. 10 (2022) 2946–2967.
[8] A.G. Olabi, E.T. Sayed, Developments in Hydrogen, Fuel Cells 16 (2023) 2431.
[9] C. Martínez de León, C. Ríos, P. Molina, J.J. Brey, Levelized cost of storage (LCOS) for a hydrogen system, Int. J. Hydrog. Energy 52 (2024) 1274–1284.
[10] A.G. Olabi, As bahri, A.A. Abdelghafar, A. Baroutaji, E.T. Sayed, A.H. Alami, et al., Large-vscale hydrogen production and storage technologies: Current status and future directions, Int. J. Hydrog. Energy 46 (2021) 23498–23528.
[11] A. Ajanovic, A. Glatt, R. Haas, Prospects and impediments for hydrogen fuel cell buses, Energy 235 (2021) 121340.
[12] P. Preuster, A. Alekseev, P. Wasserscheid, Hydrogen storage technologies for future energy systems, Annu. Rev. Chem. Biomol. Eng. 8 (2017) 445–471.
[13] F. Rahim Malik, H.-B. Yuan, J.C. Moran, N. Tippayawong, Overview of hydrogen production technologies for fuel cell utilization, Engineering Science and Technology, an International Journal. 43 (2023) 101452.
[14] S.P. Shet, S. Shanmuga Priya, K. Sudhakar, M. Tahir, A review on current trends in potential use of metal-organic framework for hydrogen storage, Int. J. Hydrog. Energy 46 (2021) 11782–11803.
[15] G. Mazzucco, G. Xotta, V.A. Salomoni, M. Giannuzzi, C.E. Maiorana, Solid thermal storage with PCM materials. Numerical investigations, Appl. Therm. Eng. 124 (2017) 545–559.
[16] S.D. Lewis, P. Chippar, Analysis of heat and mass transfer during charging and discharging in a metal hydride - phase change material reactor, J Energy Storage 33 (2021) 102108.
[17] M. Maggini, A.L. Facci, G. Falcucci, S. Ubertini, Numerical modeling of metal hydride-phase change material hydrogen storage systems with increased heat exchange surface area, Appl. Energy 378 (2025) 124725.
[18] S. Mellouli, F. Askri, E. Abhilash, S. Ben Nasrallah, Impact of using a heat transfer fluid pipe in a metal hydride-phase change material tank, Appl. Therm. Eng. 113 (2017) 554–565.
[19] A. Miled, S. Mellouli, H. Ben Maad, F. Askri, Improvement of the performance of metal hydride pump by using phase change heat exchanger, Int. J. Hydrog. Energy 42 (2017) 26343–26361.
[20] H. Jiang, Z. Ding, Y. Li, G. Lin, S. Li, W. Du, et al., Hierarchical interface engineering for advanced magnesium-based hydrogen storage: Synergistic effects of structural design and compositional modification, Chem. Sci. 16 (2025) 7610–7636.
[21] A. Singh, M.P. Maiya, Murthy S. Srinivasa, Experiments on solid state hydrogen storage device with a finned tube heat exchanger, Int. J. Hydrog. Energy 42 (2017) 15226–15235.
[22] G. Atalmis, S. Toros, B. Timurkutluk, Y. Kaplan, Effect of expanded natural graphite addition and copper coating on reaction kinetics and hydrogen storage characteristics of metal hydride reactors, Int. J. Hydrog. Energy 53 (2024) 647–656.
[23] U.R. Singh, S. Bhogilla, Performance analysis of LaNi5 added with expanded natural graphite for hydrogen storage system, Int. J. Hydrog. Energy 48 (2023) 21466–21475.

[24] Y. Ye, Y. Yue, J. Lu, J. Ding, W. Wang, J. Yan, Enhanced hydrogen storage of a LaNi5 based reactor by using phase change materials, Renew. Energy 180 (2021) 734–743.
[25] Z. Ding, H. Li, L. Shaw, New insights into the solid-state hydrogen storage of nanostructured LiBH4-MgH2 system, Chem. Eng. J. 385 (2020) 123856.
[26] V. Pandey, K.V. Krishna, M.P. Maiya, Numerical modelling and heat transfer optimization of large-scale multi-tubular metal hydride reactors, Int. J. Hydrog. Energy 48 (2023) 16020–16036.
[27] J. Wang, M. Dai, J. Liu, Z. Wu, Z. Zhang, J.G. Novaković, et al., A novel design for fin profile in metal hydride reactor towards heat transfer enhancement: Theoretical derivations and analysis, J Energy Storage 72 (2023) 108570.
[28] K.V. Krishna, V. Pandey, M.P. Maiya, Bio-inspired leaf-vein type fins for performance enhancement of metal hydride reactors, Int. J. Hydrog. Energy 47 (2022) 23694–23709.
[29] A.P. Shrivastav, P.K. Kanti, G. Mohan, M.P. Maiya, Design and optimization of metal hydride reactor with phase change material using fin factor for hydrogen storage, J Energy Storage 77 (2024) 109975.
[30] P.K. Kanti, A.P. Shrivastav, P. Sharma, M.P. Maiya, Thermal performance enhancement of metal hydride reactor for hydrogen storage with graphene oxide nanofluid: Model prediction with machine learning, Int. J. Hydrog. Energy 52 (2024) 470–484.
[31] G. Atalmis, K. Sattarkhanov, R.N. Kaplan, M. Demiralp, Y. Kaplan, The effect of powder and pellet forms of added metal hydride materials on reaction kinetics and storage, Int. J. Hydrog. Energy 75 (2024) 98–105.
[32] S.N. Nyamsi, I. Tolj, S. Pasupathi, Multi-objective optimization of a metal hydride reactor coupled with phase change materials for fast hydrogen sorption time, J Energy Storage 71 (2023) 108089.
[33] L. Tong, J. Xiao, T. Yang, P. Bénard, R. Chahine, Complete and reduced models for metal hydride reactor with coiled-tube heat exchanger, Int. J. Hydrog. Energy 44 (2019) 15907–15916.
[34] A. Chibani, S. Merouani, C. Bougriou, L. Hamadi, Heat and mass transfer during the storage of hydrogen in LaNi5-based metal hydride: 2D simulation results for a large scale, multi-pipes fixed-bed reactor, Int. J. Heat Mass Transf. 147 (2020) 118939.
[35] S.A. Mostafavi, Z. Hajabdollahi, A. Ilinca, Multi-objective optimization of metal hydride hydrogen storage tank with phase change material, Thermal Science and Engineering Progress. 36 (2022) 101514.
[36] A. Chibani, C. Bougriou, S. Merouani, Simulation of hydrogen absorption/desorption on metal hydride LaNi5-H2: Mass and heat transfer, Appl. Therm. Eng. 142 (2018) 110–117.
[37] H. Chang, Y.B. Tao, W.Y. Wang, Numerical study on storage performance of metal hydride reactors with multiple spiral fins, Int. J. Hydrog. Energy 48 (2023) 35170–35184.
[38] A. Singh, M.P. Maiya, S.S. Murthy, Effects of heat exchanger design on the performance of a solid state hydrogen storage device, Int. J. Hydrog. Energy 40 (2015) 9733–9746.
[39] J. Yuan, M. Yao, B. Zhao, Y. Lv, H. Huang, J. Chen, et al., Influence of heat exchanger structure on hydrogen absorption-desorption performance of hydrogen storage vessel, Prog. Nat. Sci. Mater. Int. 32 (2022) 617–624.
[40] J. Yao, P. Zhu, C. Qian, U. Hamidullah, S. Kurko, F. Yang, et al., Study of an autothermal-equilibrium metal hydride reactor by reaction heat recovery as hydrogen source for the application of fuel cell power system, Energy Convers. Manag. 213 (2020) 112864.
[41] M. Afzal, P. Sharma, Design and computational analysis of a metal hydride hydrogen storage system with hexagonal honeycomb based heat transfer enhancements-part a, Int. J. Hydrog. Energy 46 (2021) 13116–13130.
[42] D. Wang, Y. Wang, F. Wang, S. Zheng, S. Guan, L. Zheng, et al., Hydrogen storage in branch mini-channel metal hydride reactor: Optimization design, sensitivity analysis and quadratic regression, Int. J. Hydrog. Energy 46 (2021) 25189–25207.
[43] A. Karmakar, A. Mallik, N. Gupta, P. Sharma, Studies on 10kg alloy mass metal hydride based reactor for hydrogen storage, Int. J. Hydrog. Energy 46 (2021) 5495–5506.
[44] Z.-Y. Dai, P. Wu, L.-R. Xiao, H. Kimura, C.-X. Hou, X.-Q. Sun, et al., Non-stoichiometric $Ni_3ZnC_{0.7}$ carbide loading on melamine sponge-derived carbon for hydrogen storage performance improvement of MgH2, Rare Metals 44 (2025) 515–530.
[45] Z.-Y. Li, L.-X. Sun, F. Xu, Y.-M. Luo, Y.-P. Xia, S. Wei, et al., Modulated noble metal/2D MOF heterostructures for improved hydrogen storage of MgH2, Rare Metals 43 (2024) 1672–1685.
[46] A. Jemni, S.B. Nasrallah, J. Lamloumi, Experimental and theoretical study of ametal–hydrogen reactor, Int. J. Hydrog. Energy 24 (1999) 631–644.
[47] H.-Y. Deng, L.-J. Jiang, S.-H. Wang, W.-Q. Jiang, Y.-F. Wu, X.-M. Guo, et al., Efficient hydrogen transfer carriers: Hydrogenation mechanism of dibenzyltoluene catalyzed by Mg-based metal hydride, Rare Metals 44 (2025) 2118–2127.
[48] H. Yang, Z. Ding, Y.-T. Li, S.-Y. Li, P.-K. Wu, Q.-H. Hou, et al., Recent advances in kinetic and thermodynamic regulation of magnesium hydride for hydrogen storage, Rare Metals 42 (2023) 2906–2927.
[49] F. Bouzgarrou, F. Askri, S. Mellouli, S. Algarni, Numerical investigation of heat and mass transfer within different configurations of LaNi5–H2 reactor using the unstructured lattice Boltzmann method, Int. J. Hydrog. Energy 44 (2019) 31216–31229.